 doi:10.20944/preprints201907.0096.v1

The Effects of Hot Deformation Parameters on the Size of Dynamically Recrystallised Austenite Grains of HSLA Steel

Sebastian Gnapowski [1]*, Elżbieta Kalinowska-Ozgowicz[2] , Mariusz Śniadkowski [3], Aleksandra Pietraszek [4]

Lublin University of Technology, Fundamentals of Technology Faculty; kalinowska-ozgowicz@tlen.pl (E. K. O.); m.sniadkowski@pollub.pl (M. S.); aleksandra.pietraszek@op.pl (A. P.)

* Correspondence: sgnapowski@wp.pl

Abstract

This paper presents the results of investigations of the effects of hot deformation parameters in compression investigation on the austenite grain size in HSLA steel (0.16% C, 0.037% Nb, 0.004% Ti, 0.0098% N). The axisymmetric compression investigations were performed on cylindrical investigation specimens of d=1.2 using the Gleeble 3800 simulator [1–2]. The strain rate=$1s^{-1}$÷$15.9s^{-1}$ and strain degree ε=1.2. Before deformation, the research specimens were austenitized at T_A = 1100 ÷ 1250 °C. Metallographic observations of the primary austenite grains were conducted with an optical microscope, while the structure of dynamically recrystallized austenite, inherited by martensite, was examined by EBSD technique using a scanning electron microscope. Based on the analysis of investigation results, it was found that the size of dynamically recrystallized austenite grains in HSLA steel were clearly affected by hot compression parameters. In contrast, no significant impact of austenitising temperature on their size was found [3–4].

Keywords: HSLA steel, dynamic recrystallization, austenite grain, plastic strain, Gleeble simulator

1. Introduction

Dynamic recrystallization takes place during high-temperature deformation with the materials in which dynamic recovery does not largely occur and does not reduce the formation of structure with emerging and migrating recrystallization fronts. Metallurgical cleanness and chemical composition of the investigated materials has a significant influence on the plastic strain process under such conditions. The alloying elements affect both the recovery process and the dynamic recrystallization process. However, a distinction between the elements dissolved in solid solution and those that form the second phase particles should be made.

Generally, alloying elements in solutions reduce the recovery rate by lowering their EBU and segregating to dislocations, thereby hindering the cross slip section, climbing and unwinding of dislocation nodes. This results in a rapid increase in the dislocation density, thus providing high propelling force for dynamic recrystallization as well as for rapid work hardening. Therefore, dissolved alloying elements or micro-additions of such elements affect the dynamic recrystallization by modifying a substructure formed at the dynamic recovery stage, the interactions with dislocations during the formation of recrystallization fronts and the interaction with migrating recrystallization fronts.

Presumably, the alloying elements that significantly reduce EBU and whose interactions with recrystallization fronts are minimal facilitate this process. Slight amounts of impurities in microalloyed steels have much stronger impact on migration of recrystallization fronts than on dynamic recovery. Such effects and factors that occur in microalloyed steels (HSLA) during hot deformation have just a significant impact on grain size of austenite inherited by the structures of transformation after cooling, affecting as a consequence the performance of steel [3-6].

Preprints (www.preprints.org) | NOT PEER-REVIEWED | Posted: 8 July 2019 doi:10.20944/preprints201907.0096.v1

In microalloyed steels, the effect of second phase particles on dynamic recrystallization depends on their size, shape and distribution in the matrix. If the secondary phase particles are fine and of high dispersion, they stabilise substructure, hinder the formation of recrystallization fronts and their migration and inhibit dynamic recovery. As a result, the impact of such particles inhibits dynamic recrystallization and may result in significant grain refining. In contrast, when the second phase particles are precipitated within the grain boundaries, they can effectively block their migration, that is inhibit dynamic recrystallization without significantly affecting dynamic recovery.

For large second phase particles that interact with dislocations as stress concentrators and at the same time are privileged points for heterogeneous formation of recrystallization nucleus, the acceleration of dynamic recrystallization is observed.

Table 1. Chemical composition of HSLA steel under investigation

Element concentrations, wt%									
C	Mn	Si	P	S	Ti	Nb	V	Al	N
0.16	1.48	0.29	0.030	0.017	0.004	0.037	0.002	0.010	0.0098

Hot deformation parameters have a decisive impact on the formation of secondary phases of micro-additions that determine the course of dynamic recrystallization and structure refinement in HSLA steels [7-9]. Many strategies have been adopted to improve the ductility and impact properties of these ultrahigh strength DP steels, such as refining microstructure, alloying, design of new processing methods [10-12]. HSLA steel has better mechanical properties, including high strength, better corrosion resistance than carbon steel [13-17]. Mechanical properties are usually controlled by chemical substances composition and thermo-mechanical treatments [18-24]. Nevertheless, they are often observed with various factors of the final mechanical properties. The mechanical properties are strongly dependent on the fraction of reverted austenite which is very sensitive to the heat treatment [25–29].

2. Materials and Methods

The investigations were carried out on HSLA (High Strength Low Alloy) steel from the industrial process with chemical composition as in (Table 1).

Plastometric investigations by axisymmetric hot compression method were carried out for HSLA steel to determine the effect of the austenitising temperature as well as the strain temperature, degree and rate on the σ-ε flow curves, which represent thermally activated processes that take place in the material being deformed and determine the change in structure, in particular with regard to the size of austenite grain. The axisymmetric hot compression investigations were carried out on cylindrical research specimens of 7 mm in diameter and 8.4 mm in length using Gleeble 3800 simulator.

The research specimens were heated in the simulator by resistance method, in argon atmosphere. To reduce the coefficient of friction, the investigations specimen faces were coated with graphite and tantalum foil. Continuous compression researches to $\varepsilon = 1.2$ were carried out on researches specimens austenitized in a temperature range of 1100÷1250 °C and deformed in a temperature range of 800÷1250 °C at a strain rate (ε^{o}) of approx. $1.0s^{-1}$, $3.6s^{-1}$, $9.55s^{-1}$ and $15.9s^{-1}$. Immediately after the compression investigation, the research specimens were cooled in water to freeze the effects of hot plastic deformation. Metallographic microscopic examinations were carried out on longitudinal microsections of hot compressed and water- or air-cooled reseach specimens.

Preprints (www.preprints.org) | NOT PEER-REVIEWED | Posted: 8 July 2019 doi:10.20944/preprints201907.0096.v1

Structure observations were made with Olympus GX71 microscope (Japan) at magnifications of up to approx 2000x and optionally in polarised light. To reveal the primary austenite grains, the etching with saturated aqueous solution of picric acid at 70 °C was used. In other cases, the microsections were etched with a reagent (nital). The measurement of average diameter of the primary austenite grain was taken normatively by counting the number of intersections on minimum seven representative fields of observation. The results of measurements were developed statistically for confidence interval of P=0.95. The examinations by EBSD technique were carried out to characterise the structure of austenite inherited by martensite by using a scanning electron microscope Inspect F with a Schottky field emission gun. The research specimens for EBSD examinations were prepared conventionally by mechanical grinding and polishing with water-based suspension of Al_2O_3 with grain size of 0.1 μm.

In the final stage of preparation, the specimens were ion polished with Gatan 682 system.

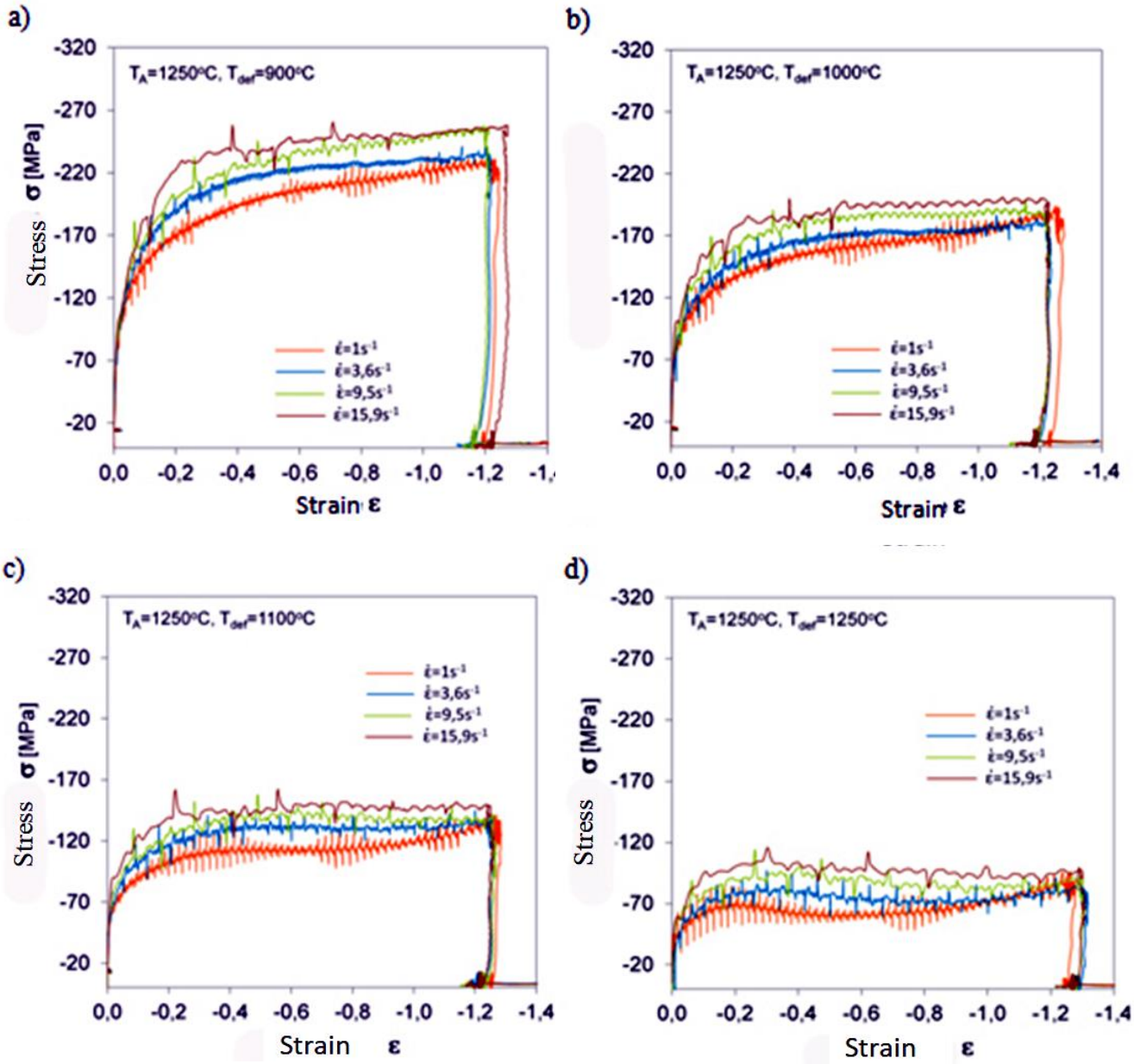

Figure 1. The effect of strain temperature and strain rate in compression investigation on flow curves of the investigated steel austenitized at 1250 °C, T_{def} a) 900 °C, b) 1000 °C, c) 1100 °C, d) 1250V

Preprints (www.preprints.org) | NOT PEER-REVIEWED | Posted: 8 July 2019 doi:10.20944/preprints201907.0096.v1

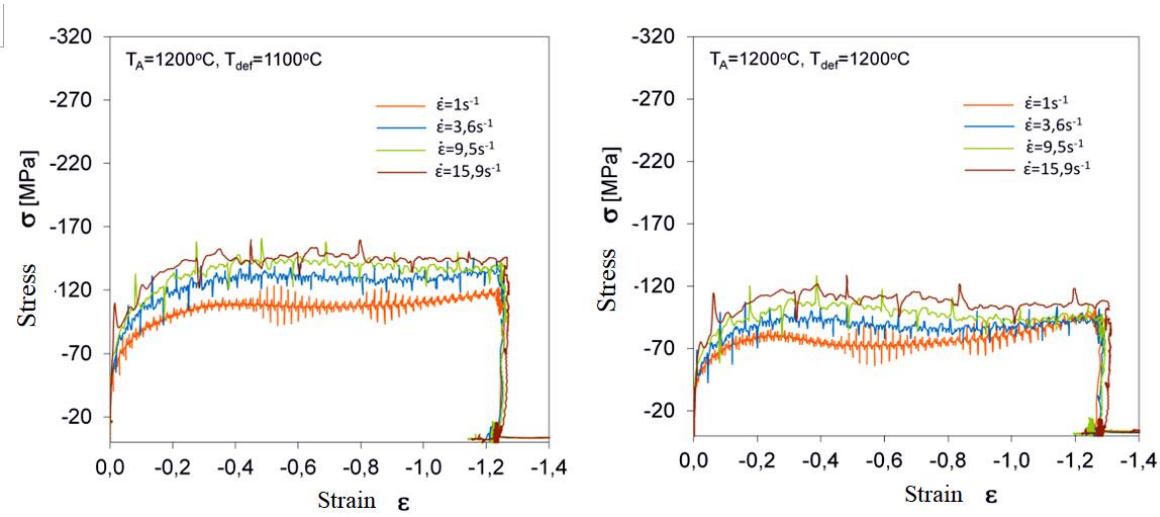

Figuer 2. The effect of strain temperature and strain rate in compression investigation on flow curves of HSLA steel austenitized at 1200 °C, T_{def} a) 1100 °C, b) 1200 °C

3. Results

The investigated microalloyed steel with Ti, Nb and N deformed in high-temperature compression investigation to ε=1.2 reveals flow curves of different waveforms, dependent mainly on the austenitising temperature as well as the strain temperature and rate (Figure 1).

After austenitizing at T_A = 1250 °C and 1200 °C and deformation in a temperature range of T_{def} = 1100÷1250 °C at a rate between 1.0s^{-1} and 15.9s^{-1}, the recorded σ-ε curves are characterised by the occurrence of more or less distinct maximum flow stress and a limited scope of fixed stresses, determined by the course of dynamic recrystallization (Figure 1 - 3). At a lower deformation temperature (900 and 1000 °C), dynamic recrystallization is not disclosed (Figure 1a, b), as the deformation (= 1.2) achieved in the compression investigation performed is too small to trigger the dynamic recrystallization process in the investigated steel. Under such deformation conditions, dynamic recovery is the decisive process that removes the effects of strain hardening.

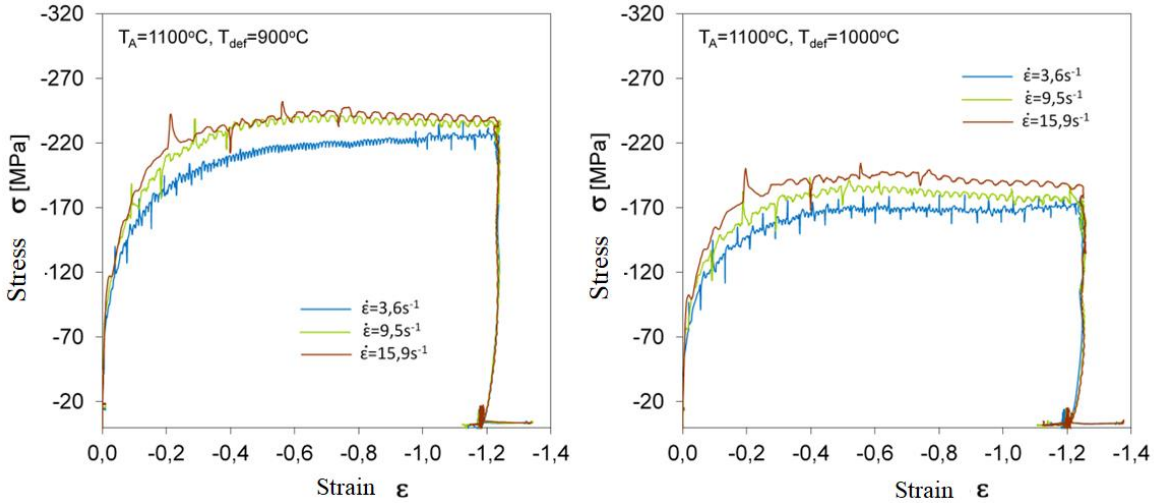

Figure 3. The effect of strain temperature and strain rate in compression investigation on flow curves of microalloyed steel austenitized at 1100 °C, T_{def} a) 90 0°C, b) 1000 °C

Preprints (www.preprints.org) | NOT PEER-REVIEWED | Posted: 8 July 2019 doi:10.20944/preprints201907.0096.v1

At a higher deformation temperature (1100÷1250°C), the σ-ε curves show a slight reduction in flow stress value as a (Figure 3). The ε_m values on the σ-ε curves decrease as the strain temperature increases and the strain rate decreases. Changes in flow stress of the investigated hot-deformed steel depend significantly on the strain temperature and strain rate, but do not depend clearly on the austenitising temperaturę within the range being investigated (1250÷1100 °C). The maximum stress values in steel after austenitising and deformation at 1200 °C increase from 78.8 MPa to 115.6 MPa with increase in the strain rate in the range between $1.0s^{-1}$ and $15.9s^{-1}$ (Figure 2b). After austenitising at 1200 °C and deformation at 1100 °C while at the same maintaining the same rate, σ_{max} values increase from 108 MPa to 151 MPa (Figure 2a).

The metallographic examinations carried out have allowed the effect of high-temperature deformation parameters on the size and shape of the primary austenite grain (d_o) before $\gamma \rightarrow \alpha'$ transition conditioned by the course of thermally activated processes to be determined. It was found that austenitising temperature had a decisive impact on the austenite grain size before high-temperature deformation (Figure 4). The investigated steel austenitised at 1100 °C reveals austenite grains of d_o = 36μm (Figure 4a). The increase in austenitising temperature up to 1200 °C and 1250 °C results in increase in the primary grain size γ up to approx. 76μm and 83μm, respectively (Figure 4c). After the steel has been cooled down from this austenitising temperature range in water, lath martensite with bainite areas (Figure 4b, d) and various lath sizes was revealed in microstructure of the investigated steel.

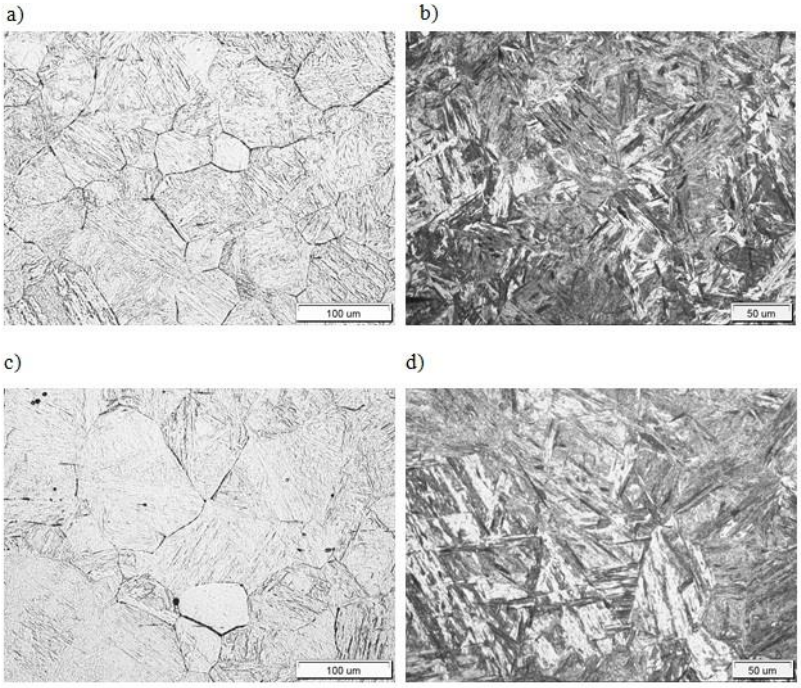

Figure 4. Structure of the investigated steel after austenitizing at a,b) 1100 °C, c,d) 1250 °C; primary austenite grain size (a,c), martensitic – bainitic structure (b,d)

Preprints (www.preprints.org) | NOT PEER-REVIEWED | Posted: 8 July 2019 doi:10.20944/preprints201907.0096.v1

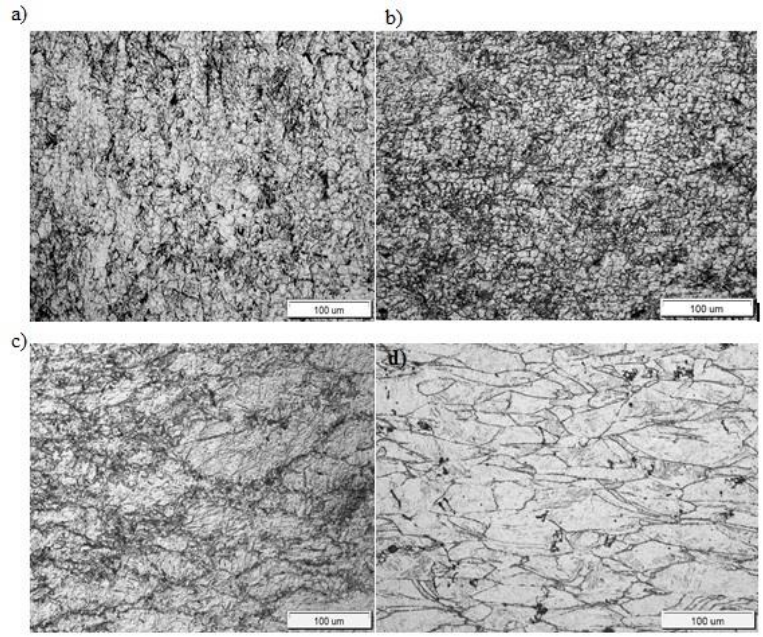

Figure 5. The effect of strain temperaturę at a strain rate = 1.0 s^{-1} on the structure of primary austenite grains of the investigated steel: a) 1200 °C, b) 1100°C, c) 1000 ° C , d) 800 °C (T_A=1200 °C, ε=1.2)

The results of metallographic observations of micro – alloys steel deformed plastically in compression investigation at a strain rate of approx. 1.0s^{-1} and a constant strain degree (ε = 1.2) in a Table 2 temperature range of 1200÷800 °C after austenitising at 1200 °C are shown in the microphotograph (Figure 5). Primary austenite grains of varying sizes and forms depending on strain temperature were revealed in the structure of HSLA steels. Deformation at 1200 °C and 1100 °C allows the dynamically recrystallised γ grains of approx. 16.1 μm (Figure 5a) and approx.10 μm (Figure 5b), respectively, to be obtained within the entire material volume (Table 2).

Table 2. Average primary austenite grain diameter

Austenitizing temperature, °C	Average γ grain diameter d_o, μm	Strain temperature, °C	Strain rate ε s^{-1}	Average γ grain diameter d, μm
1200	76.1 ±12	1200	1.0	16.1 ±2
		1100		10.0 ±1
1100	34.3 ±10	1100	3.6	9.8 ±2

The advantageous refinement effect of γ grains while maintaining their high dimensional uniformity and equiaxiality is shown clearly in the microphotograph (Figure 5b). After deformation at 1000 °C, fine recrystallised γ grains were revealed in the near-boundary areas and occasionally within the primary austenite grains as a result of the initiation of dynamic recrystallization (Figure 5c), while after deformation at 800 °C, clearly elongated primary austenite grains with a number of deformed twins and slip bands, which are characteristic of the hardening stage on σ-ε flow curves with a small contribution of thermally - activated processes, primarily dynamic recovery, were revealed (Figure 5d).

Preprints (www.preprints.org) | NOT PEER-REVIEWED | Posted: 8 July 2019 doi:10.20944/preprints201907.0096.v1

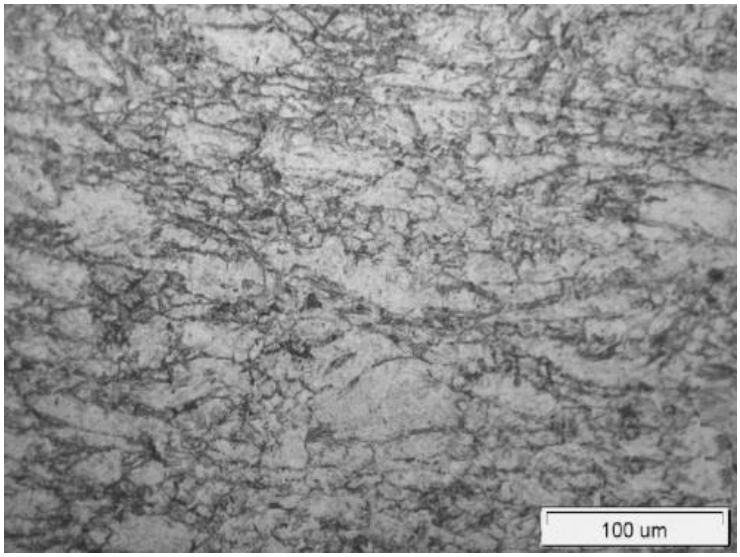

Figure 6. Partially dynamically recrystallized primary austenite grains of HSLA steel after deformation at 1000 °C and = 15.9s-1 (T_A=1250°C, ε=1.2)

The additive effect of strain temperature and strain rate in the austenitising temperature range (1250 °C, 1200 °C) on the structure of primary austenite grains of the investigated steel is shown in (Figure 6, 7). The increase in strain rate up to approx. 15.9s^{-1} causing the effect of delayed dynamic recrystallization of the investigated steel, recorded on the flow curves, affects also the microstructure of primary γ grains in the analysed strain temperature range (Figure 6). At a comparable strain temperature of 1100°C and strain degree (ε = 1.2), the primary austenite grains of the investigated steel deformed at a rate = 1.0 s^{-1} are dynamically recrystallised to a full extent (Figure 5b), while those deformed at a rate = 3.6 s^{-1} only show partial dynamic recrystallization (Figure 7a). A similar effect of changes in microstructure of primary γ grains is observed for strain temperature of 1000 °C and strain rate of 3.6s^{-1} and 15.9s^{-1} (Figure 6). In (Figure 7b), austenite after dynamic deformation(T_A=1200 °C T_{def}=900 °C, ε = 1.2,=1s^{-1}) reveals a microstructure of elongated grains with deformed twins inside them and fine dynamically recrystallized grains mostly at the boundaries of former primary austenite grains, which is a structure characteristic of the initial phase of dynamic recrystallization.

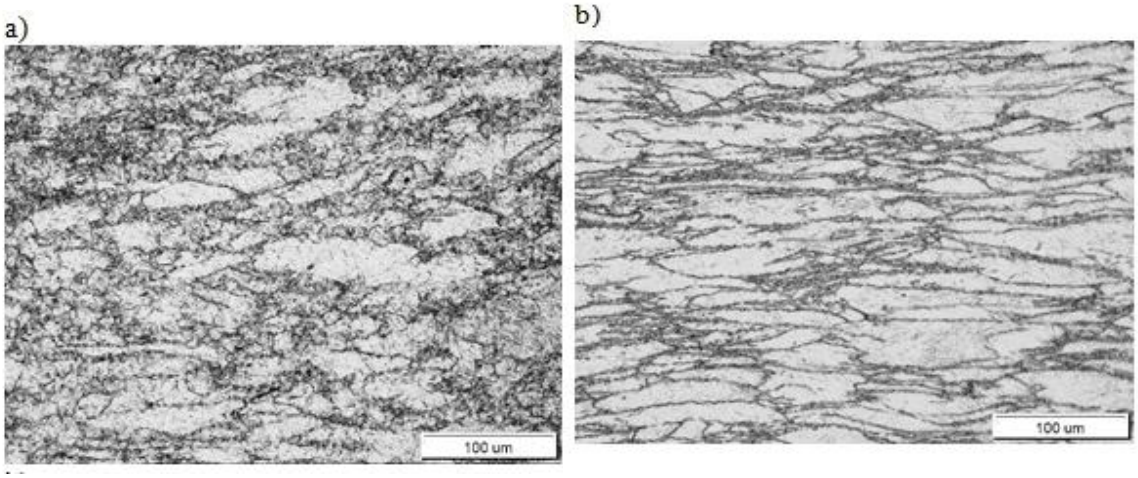

Figure 7. Partially dynamically recrystallized primary austenite grains after deformation at = 3.6 s^{-1} and: a) 1100 °C, b) 900 °C (T_A=1200°C, ε=1.2)

Preprints (www.preprints.org) | NOT PEER-REVIEWED | Posted: 8 July 2019 doi:10.20944/preprints201907.0096.v1

In the investigated steel deformed from ε = 0.268 at an austenitising temperature of 1200 °C and a rate = 1.0s^{-1}, fine recrystallised austenite grains were revealed on the background of the primary γ grains corresponding to the applied austenitising temperature (Figure 8a). Under such conditions, the strain of ε = 0.4 at 1000 °C does not initiate dynamic recrystallization yet (Figure 8b). All the more in case of a compression investigation of the investigated steel at 800 °C and 900 °C and strain degree ε=0.6 the revealed primary austenite grains only show distinct effects of strain hardening or dynamic recovery, but do not reveal the common symptoms indicating a potential contribution of dynamic recrystallization (Figure 9).

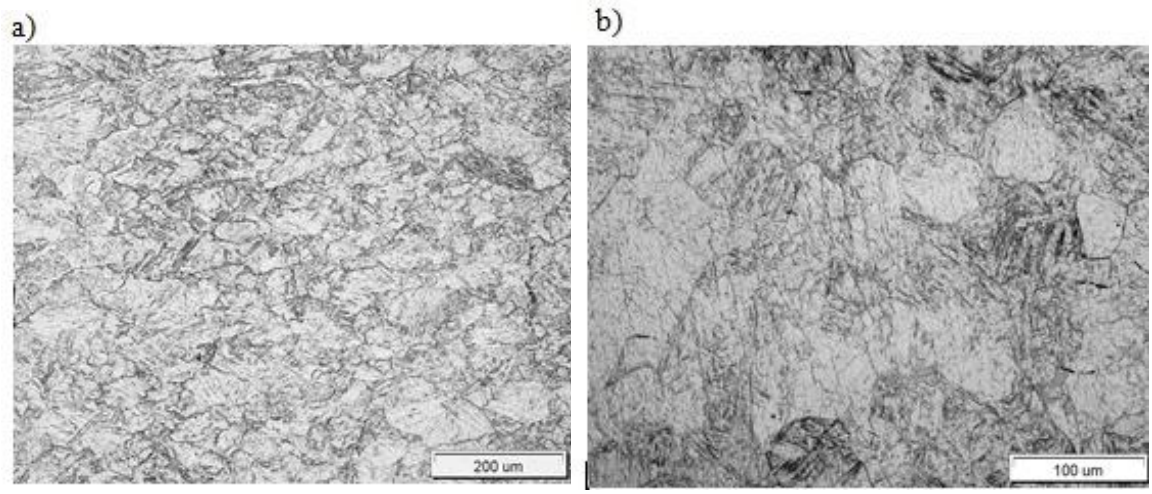

Figure 8. The effect of HSLA steel strain degree and strain temperature on the structure of primary austenite grains: a) ε = 0.268, T_{def} = 1200 °C, b) ε=0.4, T_{def} = 1000 °C (T_A=1200 °C, = 1.0s^{-1})

The austenite grain size (d) for the analysed range of strain parameters due to which the main process resulting in the reduction of hardening in HSLA steel was dynamic recrystallization is shown in Table 2.

The structure of austenite inherited by martensite in the investigated steel after compression deformation at 1000 °C and a rate of 1.0 s^{-1} (T_A= 1200 °C) is shown in the microphotograph (Figure 10). The boundaries of dynamically recrystallized austenite grains were observed on the background of martensite plates.

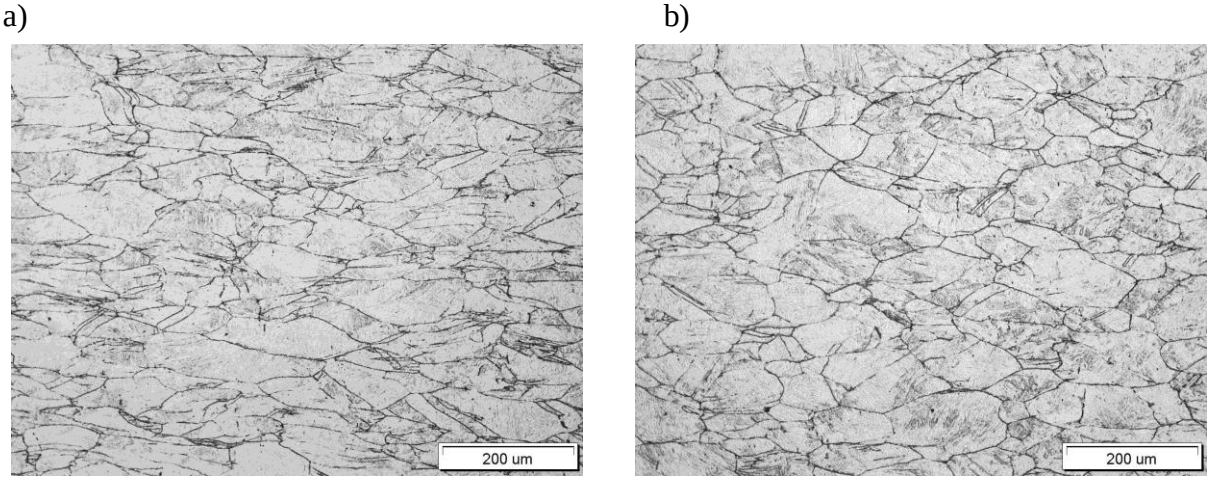

Figure 9. The effect of HSLA steel strain degree and strain temperature on the structure of primary austenite grains: a) ε = 0.6, T_{def} = 800 °C, b) ε = 0.6, T_{def} = 900°C (T_A=1200 °C, = 1.0s^{-1}), b) ε = 0,6, T_{def} = 900 ° C (T_A = 1200 ° C, = 1,0 s-1

Preprints (www.preprints.org) | NOT PEER-REVIEWED | Posted: 8 July 2019 doi:10.20944/preprints201907.0096.v1

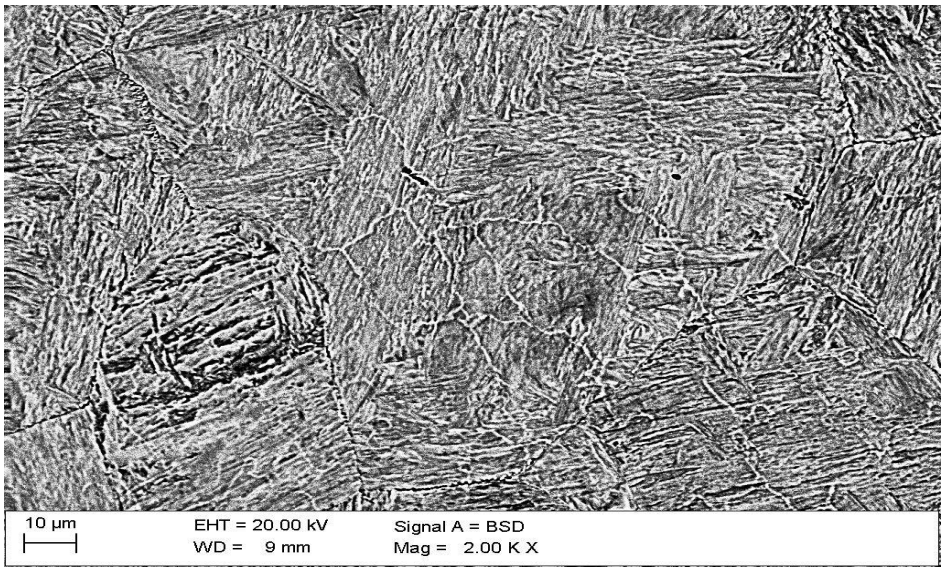

Figure 10. Structure of dynamically recrystallized austenite compared to martensite after deformation of HSLA steel at 1000 °C and a rate of $1s^{-1}$ followed by water cooling (T_A=1200 °C, ε=1.2)

The result of EBSD analysis is shown in the microphotographs (Figure 11) and charts (Figure 12, 13).

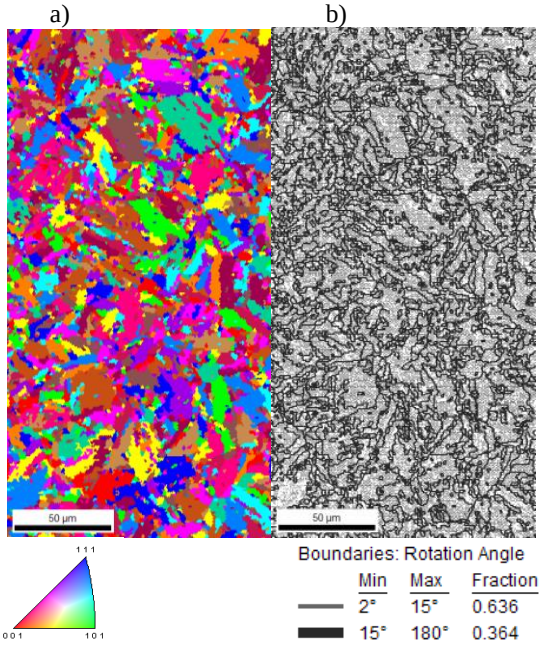

Figure 11. Result of EBSD analysis carried out for HSLA steel after deformation at 1000 °C and a rate of $1.0s^{-1}$ (T_A=1200 °C, ε=1.2/water)

Preprints (www.preprints.org) | NOT PEER-REVIEWED | Posted: 8 July 2019 doi:10.20944/preprints201907.0096.v1

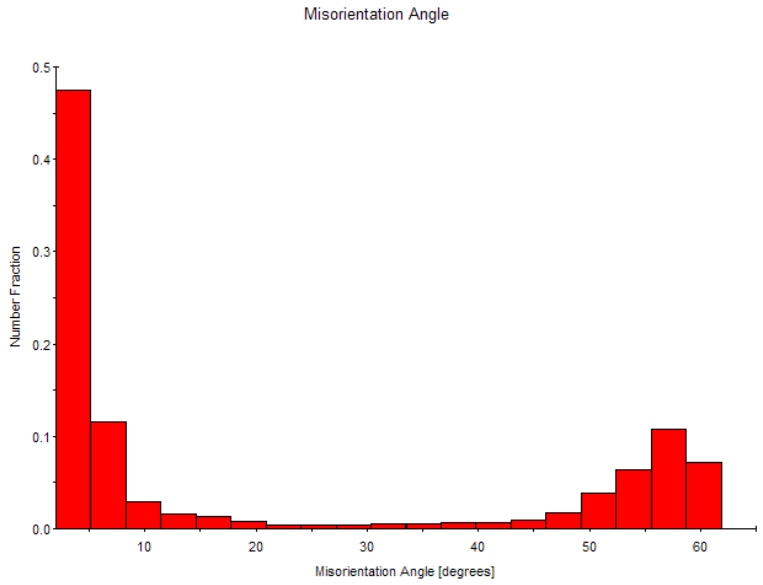

Figure 12. Grain disorientation angle distribution

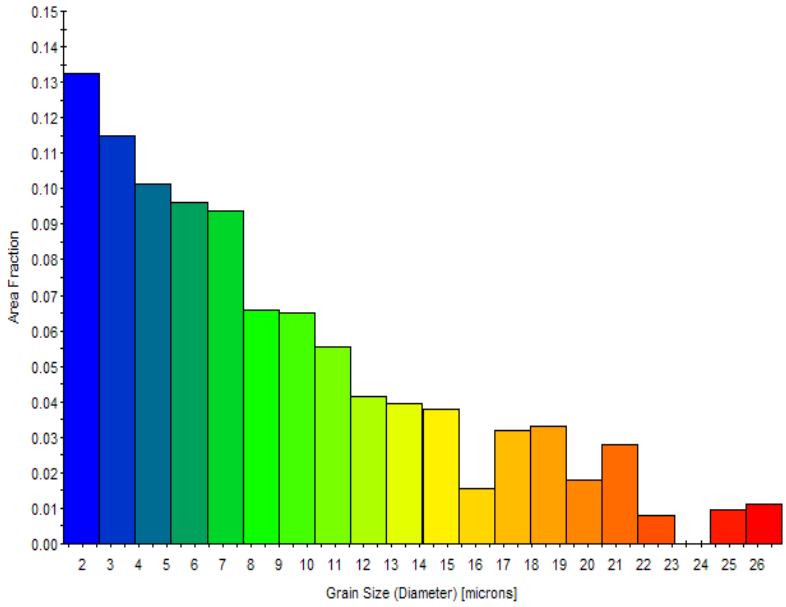

Figure 13. Grain size distribution

The microstructure resulting from deformation and hardening of HSLA steel is shown on the EBSD map with colour-coded grains oriented according to the inverse pole figure triangle (Figire 11a). The microphotograph (Figure 11b) shows a qualitative image of the map with misorientation angles of grains out of which 63.6% are characterised by low-angle boundaries with misorientation angle of 2°÷15°. Such a misorientation in microstructure is revealed by subgrains. The grain size and distribution is shown in the chart (Figure 12) and the misorientation angle distribution is shown in the chart (Figure 13).

Preprints (www.preprints.org) | NOT PEER-REVIEWED | Posted: 8 July 2019 doi:10.20944/preprints201907.0096.v1

5. Conclusions

The austenitising temperature before the γ to α' transformation have a decisive impact on the primary austenite grain size in HSLA steel. The investigated steel austenitised at 1100 °C is characterised by austenite grains with average diameter of d_o=34 μm, and after austenitising at 1200 and 1250 °C by grains of d_o=74μm and 83μm, respectively. For the investigated microalloyed steel with Ti, Nb and N, the size of dynamically recrystallised γ grain decreases as the strain temperature is lowering and is increasing. These parameters have a much greater impact on regrouping and distribution of dislocations resulting in the formation of recrystallisation fronts (grain refinement) than on the rate of their migration (grain growth). The reduction in strain temperature from 1200 to 1100 °C at austenitizing temperature of 1200 °C and strain rate of 1.0 s^{-1} allowed the γ grain size to be reduced from approx. 16μm to approx. 10μm. The increase in strain rate up to = 3.6 s^{-1} at a strain temperature and an austenitising temperature of 1100 °C has resulted in the reduction in austenite grain size to d=9.8 μm in HSLA steel.

The grain size obtained during dynamic recrystallization does not depend on the primary grain size obtained during austenitizing in the analysed temperature range (1100÷1250 °C).

References

1. Ozgowicz W., Opiela M., Kalinowska-Ozgowicz E., Metallurgical products of microalloy constructional steels, Journal of Achievements in Materials and Manufacturing Engineering, 44, 1, **2011**, 7-19.
2. Kalinowska-Ozgowicz E., Kuziak R., Ozgowicz W., Lenik K., Kinetics of the precipitation in austenite HSLA steels, nr 5, vol. 49, **2015**, 673-679.
3. Kalinowska-Ozgowicz E., Wajda W., Ozgowicz W., Mathematical modelling and physical simulation of the hot plastic deformation and recrystallization of steel with micro-additives, Materiali in Tehnologije, nr 1, vol. 49, **2015**, 69-74.
4. Kalinowska - Ozgowicz E., Structural and mechanical factors of the strengthening and recrystallization of hot plastic deformation of steels with microadditives, (in Polish), Open\Acces Library vol.20, URLhttp://www.openaccesslibrary.com/index.php?id=97, **2013**, 1-246.
5. Kuziak R., Modeling changes in structure and phase transformations occurring in the processes treatment of thermo-plastic steel, Instytut Metalurgii Żelaza (in Polish) Gliwice **2005**.
6. Roberts W., Boden H., Ahblo B., Dynamic recrystallization kinetics, Metal Science.,13, 3/4, **1979**. 195-205.
7. Skobir D. A., High-strength low-alloy (HSLA) steels, Materials and Technology, 45, **2011**, 4, 295-301.
8. Adamczyk J., Kalinowska-Ozgowicz E., Ozgowicz W., R. Wusatowski R., Interaction of carbonitrides V(CN) undissolved in austenite on the structure and mechanical properties of microalloyed V-N Steels, Journal of Materials Processing Technology, 53, **1995**, 23-32.
9. Adamczyk J., Ozgowicz W.**,** Wusatowski R., Kalinowska-Ozgowicz E., Grzyb R., Boron treated microalloyed quenched and tempered plates, their structure and properties, Journal of Materials Processing Technology, 64, **1997**, 1-8.
10. Mazaheri, Y.; Kermanpur, A.; Najafizadeh, A. Microstructures, mechanical properties, and strain hardening behavior of an ultrahigh strength dual phase steel developed by intercritical annealing of cold-rolled ferrite/martensite. Metall. Mater. Trans. A **2015**, 46, 3052–3062.
11. Ashrafi, H.; Shamanian, M.; Emadi, R.; Saeidi, N. A novel and simple technique for development of dual phase steels with excellent ductility. Mater. Sci. Eng. A **2017**, 680, 197–202.
12. Kalashami, A.G.; Kermanpur, A.; Najafizadeh, A.; Mazaheri, Y. Development of a high strength and ductile Nb-bearing dual phase steel by cold-rolling and intercritical annealing of the ferrite-martensite microstructures. Mater. Sci. Eng. A **2016**, 658, 355–366.
13. Zepon, G.; Nascimento, A.R.C.; Kasama, A.H.; Nogueira, R.P.; Kiminami, C.S.; Botta, W.J.; Bolfarini, C. Design of wear resistant boron-modified supermartensitic stainless steel by spray forming process. Mater. Des. **2015**, 83, 214–223.

14. Della Rovere, C.A.; Ribeiro, C.R.; Silva, R.; Baroni, L.F.S.; Alcântara, N.G.; Kuri, S.E. Microstructural and mechanical characterization of radial friction welded supermartensitic stainless steel joints. Mater. Sci. Eng. A **2013**, 586, 86–92.
15. Deleu, E.; Dhooge, A. Weldability Assessment of Thick Super-Martensitic 13Cr Stainless Steel Welds Made with Matching Consumables. Weld. World **2005**, 49, 34–44.
16. Aquino, J.M.; Rovere, C.A.D.; Kuri, S.E. Localized Corrosion Susceptibility of Supermartensitic Stainless Steel inWelded Joints. Corrosion **2008**, 64, 35–39.
17. Anselmo, N.; May, J.E.; Mariano, N.A.; Nascente, P.A.P.; Kuri, S.E. Corrosion behavior of supermartensitic stainless steel in aerated and CO2-saturated synthetic seawater. Mater. Sci. Eng. A **2006**, 428, 73–79.
18. De Sanctis, M.; Lovicu, G.; Valentini, R.; Dimatteo, A.; Ishak, R.; Migliaccio, U.; Montanari, R.; Pietrangeli, E. Microstructural Features Affecting Tempering Behavior of 16Cr–5Ni Supermartensitic Steel. Metall. Mater. Trans. A **2015**, 46, 1878–1887.
19. Ma, X.;Wang, L.; Subramanian, S.V.; Liu, C. Studies on Nb Microalloying of 13Cr Super Martensitic Stainless Steel. Metall. Mater. Trans. A **2012**, 43, 4475–4486.
20. Ye, D.; Li, J.; Jiang, W.; Su, J.; Zhao, K. Effect of Cu addition on microstructure and mechanical properties of 15% Cr super martensitic stainless steel. Mater. Des. **2012**, 41, 16–22.
21. Lian, Y.; Huang, J.; Zhang, J.; Zhang, C.; Gao,W.; Zhao, C. Effect of 0.2 and 0.5% Ti on the microstructure and mechanical properties of 13Cr supermartensitic stainless steel. J. Mater. Eng. Perform. **2015**, 24, 4253–4259.
22. Escobar, J.D.; Poplawsky, J.D.; Faria, G.A.; Rodriguez, J.; Oliveira, J.P.; Salvador, C.A.F.; Mei, P.R.; Babu, S.S.; Ramirez, A.J. Compositional analysis on the reverted austenite and tempered martensite in a Ti-stabilized supermartensitic stainless steel: Segregation, partitioning and carbide precipitation. Mater. Des. **2018**, 140, 95–105.
23. Rodrigues, C.A.D.; Bandeira, R.M.; Duarte, B.B.; Tremiliosi-Filho, G.; Jorge, A.M. Effect of phosphorus content on the mechanical, microstructure and corrosion properties of supermartensitic stainless steel. Mater. Sci. Eng. A **2016**, 650, 75–83.
24. Silva, G.F.; Tavares, S.S.M.; Pardal, J.M.; Silva, M.R.; de Abreu, H.F.G. Influence of heat treatments on toughness and sensitization of a Ti–alloyed supermartensitic stainless steel. J. Mater. Sci. **2011**, 46, 7737–7744.
25. Nakagawa, H.; Miyazaki, T. Effect of retained austenite on the microstructure and mechanical properties of martensitic precipitation hardening stainless steel. J. Mater. Sci. **1999**, 34, 3901–3908.
26. Leem, D.S.; Lee, Y.D.; Jun, J.H.; Choi, C.S. Amount of retained austenite at room temperature after reverse transformation of martensite to austenite in an Fe–13%Cr–7%Ni–3%Si martensitic stainless steel Scripta Mater. **2001**, 45, 767–772.
27. Akhavan, B.; Ashrafizadeh, F.; Hassanli, A.M. Influence of Retained Austenite on the Mechanical Properties of Low Carbon Martensitic Stainless Steel Castings. ISIJ Int. **2011**, 51, 471–475.
28. Song, Y.Y.; Li, X.Y.; Rong, L.J.; Li, Y.Y.; Nagai, T. Reversed austenite in 0Cr13Ni4Mo martensitic stainless steels. Mater. Chem. Phys. **2014**, 143, 728–734.
29. Bojack, A.; Zhao, L.; Morris, P.F.; Sietsma, J. Austenite Formation from Martensite in a 13Cr6Ni2Mo Supermartensitic Stainless Steel. Metall. Mater. Trans. A **2016**, 47, 1996–2009.